Available online at www.sciencedirect.com
SCIENCE DIRECT®
Biomaterials 25 (2004) 3389–3398
Biomaterials
www.elsevier.com/locate/biomaterials

A study of the nanostructure and tensile properties of ultra-high molecular weight polyethylene

Mary Beth Turell, Anuj Bellare*

Department of Orthopaedic Surgery, Brigham and Women's Hospital, Harvard Medical School, 75 Francis Street, MRB 106, Boston, MA 02115, USA

Received 31 March 2003; accepted 25 September 2003

Abstract

Ultra-high molecular weight polyethylene (UHMWPE) has gained worldwide acceptance as a bearing material used in orthopaedic implants. Despite its widespread use, inherent properties of the polymer continue to limit the wear resistance and the clinical lifespan of implanted knee and hip prosthetics containing UHMWPE components. The degree of crystallinity of UHMWPE is known to strongly influence several of its tensile mechanical properties such as Young's modulus, yield stress, strain-hardening rates, work of fracture and ultimate tensile properties. In this study, medical grade UHMWPE was subjected to four different crystallization conditions resulting in UHMWPE with a range of crystalline morphologies. Thereafter, the crystalline nanostructure was quantitatively characterized using a combination of ultra-small angle X-ray scattering and differential scanning calorimetry. Low-voltage scanning electron microscopy was employed as a supplementary technique to compare the crystalline morphology resulting from each crystallization condition. In addition, uniaxial tensile tests were performed to assess the effects of crystallization conditions on the mechanical properties of UHMWPE. This study showed that while crystallization conditions strongly influenced the morphology of UHMWPE, in most cases the mechanical properties of the material were not significantly affected.

Keywords: Polyethylene; Joint replacement; Mechanical properties; Crystallinity; SEM

1. Introduction

Ultra-high molecular weight polyethylene (UHMWPE) has gained worldwide acceptance as a bearing material used in total knee and hip joint replacement prostheses since its introduction as an orthopaedic implant material over four decades ago. Despite its widespread use, the tribological and mechanical properties of the polymer continue to limit the clinical lifespan of implanted knee and hip prosthetics containing UHMWPE components.

The objective of this structure-property study was to explore the effects of crystallization conditions on the crystalline morphology of UHMWPE with the ultimate goal of identifying specific thermal histories that would yield UHMWPE with both superior mechanical properties and wear performance. The dual-phase crystalline and amorphous structure of UHMWPE has previously been characterized using small-angle X-ray scattering (SAXS) and low-voltage scanning electron microscopy (LVSEM). UHMWPE crystalline lamellae have been shown to be in the thickness range of 10–50 nm and with lengths of approximately 10–50 μm [1]. SAXS measurements have shown the typical spacing between adjacent lamellae (inter-lamellar spacing) to be approximately 50 nm [2]. The crystalline structure of UHMWPE is influenced by molecular structure (type of branching and degree of branching), as well as by molecular weight, molecular weight distribution, and by fabrication conditions (pressure, temperature, time) [3]. The combination of these factors influences the crystallization kinetics of the polymer, which in turn control morphology [4]. The semicrystalline structure of UHMWPE provides possibilities for the modification of both the crystalline and amorphous regions in order to influence the macroscopic properties of UHMWPE and to produce a material that fully takes advantage of the optimal properties of both regions.

It is well known that crystalline morphology has a strong influence on a polymer's mechanical properties such as Young's modulus, yield stress, strain hardening rates, work of fracture (WOF) and ultimate tensile

*Corresponding author. Tel.: +1-617-732-5864; fax: 001-617-732-6705.
E-mail address: anuj@alum.mit.edu (A. Bellare).

0142-9612/$ - see front matter © 2003 Elsevier Ltd. All rights reserved.
doi:10.1016/j.biomaterials.2003.10.027

properties. Truss et al. [5] showed that for UHMWPE, the modulus varied as a function of cooling rate from the melt temperature (133°C). Under conditions of rapid cooling (quenching), the driving force for crystallization is reduced, resulting in a material with an overall lower crystallinity and a higher nucleation density [6]. In contrast, slow cooling or isothermal crystallization at low undercooling temperatures increases the overall degree of crystallinity and yields a lower nucleation density, leading to a smaller number of thick lamellae compared to quenched polyethylene. The thickness of crystalline lamellae increases with the steady increase in annealing temperature [7–9]. Improvements in mechanical properties may be attributed to differences in the quantity and morphology of the crystalline regions within UHMWPE [1]. Manufacture of UHMWPE involves either ram extrusion or compression-moulding of UHMWPE powder. Both processes employ high temperatures and moderate pressures, followed by slow cooling and a post-processing annealing step. The close relationship between fabrication conditions and the resulting UHMWPE morphology has prompted numerous investigations into all areas of the manufacturing process from the original grade of resin powder used, to the resulting stock material, and final machining of implant components [5,10–17].

In the past, the crystalline morphology of polymers has been characterized using a scanning electron microscope (SEM) in combination with permanganic acid etching to reveal fine details of the lamellar structure [18–20]. While this form of microscopy provides a qualitative assessment of the microstructure of lamellar morphology, it is limited in its ability to provide quantitative information pertaining to these structures. In contrast, X-ray scattering techniques, in particular, ultra-small-angle X-ray scattering, (USAXS) is a useful tool in the quantitative characterization of the lamellar structure of UHMWPE. The large range of scattering angles of the USAXS camera makes it possible to measure the crystalline morphology of UHMWPE at both the nanometer and micrometer length scales. USAXS is advantageous in comparison to traditional imaging methods, such as SEM and transmission electron microscopy (TEM), in that experiments provide quantitative, three-dimensional analysis of crystalline morphology. In addition, the relatively large sampling volume of approximately 5–10 mm^3 in USAXS experiments provides superior sampling statistics compared to the aforementioned imaging methods.

In this study, medical grade UHMWPE was melted and then subjected to four different cooling sequences (crystallization conditions) in order to produce UHMWPE with a variety of crystalline morphologies. Thereafter, the morphology as well as the mechanical properties of all samples was analyzed. USAXS and differential scanning calorimetry (DSC) were used to measure lamellar thicknesses, amorphous region thicknesses, spacing between adjacent lamellae, and the surface area to volume ratio of lamellae, and also to detect voids resulting from incomplete consolidation of the UHMWPE resin powder during manufacturing processes. USAXS was also used to determine the specific internal surfaces (O_{ac}), or the area per unit volume of the interface separating crystalline and amorphous regions. LVSEM was used as a supplementary tool to provide qualitative information relating to crystalline morphology. In addition, uniaxial tensile (UT) tests were performed to assess the effect of crystallization conditions on the mechanical properties of UHMWPE. It was hypothesized that by varying the crystallization conditions of UHMWPE, that the resulting morphology of the polymer could be controlled, and that differences in mechanical properties could be attributed to variations in morphology.

2. Materials and methods

2.1. UHMWPE starting material

Commercially available, ram extruded GUR 1050 (Hoechst-Ticona, Bayport, TX) 76.2 mm (3 in) diameter rod-stock (PolyHi Solidur, Ft. Wayne, IN) was used as the starting material for all crystallization experiments. The average molecular weight of the UHMWPE was between 5.5×10^6 and 6.0×10^6 g/mol [1]. Rod-stock was sectioned into 1.5 mm thick slices. Two slices were each subjected to one of four crystallization conditions to yield enough material from which to machine mechanical test specimens and to ensure reproducibility between slice samples.

Sample preparation involved crystallization of UHMWPE by one of four heating and cooling sequences. In one experiment, UHMWPE samples were held at 170°C for 30 min and then isothermal crystallization was performed in copper chambers immersed in a silicone oil bath for 48 h at a low undercooling temperature of 120°C, which is relatively close to the melting temperature of UHMWPE. In a second experiment, samples were heated to 170°C in the silicone oil bath regulated by a precise temperature controller and thereafter slowly cooled to room temperature over a period of 3 h. In a third experiment, samples were first heated to 170°C and then immediately quenched in liquid nitrogen. In a fourth set of experiments, UHMWPE that had been first heated to 170°C, then quenched in liquid nitrogen, was furthermore subjected to isothermal crystallization at 80°C for 48 h (hereafter referred to as quench/80°C) using the silicone oil bath apparatus. Non-heat treated rod-stock served as a control.

2.2. Ultra-small-angle X-ray scattering

USAXS was performed at the UNICAT beamline of the Advanced Photon Source, Argonne National Laboratory, Argonne, IL using a Bonse-Hart ultra-small-angle scattering instrument. The beam cross-sectional area was 2.0 mm × 0.6 mm and 10 kEV X-rays were used. Data were collected in the form of absolute intensity, I (cross section, cm^{-1}), as a function of the scattering vector q (nm^{-1}) where q is defined as

$$q = (4\pi/\lambda)\sin\theta$$

such that θ equals one-half of the scattering angle, and λ is the wavelength of X-rays. An angular scattering range where $q_{min} = 0.001$ (nm^{-1}) and $q_{max} = 1.0$ (nm^{-1}) was used. All USAXS samples were 10 mm × 10 mm square specimens with 1.5 mm thickness.

2.3. Differential scanning calorimetry

DSC was performed on a Perkin Elmer Pyris instrument to determine the overall degree of crystallinity in each sample. Percent crystallinity was calculated by normalizing the heat of fusion of the sample to the heat of fusion of polyethylene crystal (293 J/g) [18]. The average of three DSC measurements from each crystallization group was used to determine the overall crystallinity of the sample. All DSC samples weighed approximately 4 mg.

2.4. Low-voltage scanning electron microscopy

A JEOL 6320FV LVSEM operating at 2 kV and a working distance of 4 mm was used to image freeze fractured surfaces of all UHMWPE samples. Prior to investigation with LVSEM, fracture surfaces were etched using a permanganic acid etching technique [14,20,21] to reveal finer details in lamellar structure. The specimens were coated with a gold–palladium coating of approximately 10 nm thickness.

2.5. Mechanical tests

UT tests were performed on all UHMWPE samples using an INSTRON 4201 tensile tester operating at a crosshead-speed of 10 mm/min. All specimens were punched from 1.5 mm thick heat-treated UHMWPE slices to conform to ASTM D638 standards for type V dog-bone configuration test specimens. Tensile tests were carried out at room temperature and a minimum of six test specimens were tested for each crystallization group evaluated. Ultimate tensile stress (UTS), true strain at break, WOF, yield stress and tensile modulus were calculated.

2.6. Statistical analysis

Statistical analysis was conducted using ANOVA with Fisher's protected least significant difference (PLSD) post-hoc test in which a p-value of less than 0.05 was used to define significance. Mechanical properties data from each crystallization group were compared against one another in order to establish the level of significance of these properties between different groups.

3. Results

3.1. Ultra-small-angle X-ray scattering

USAXS scattering intensities, I (cm^{-1}), were plotted as a function of the scattering vector, q (nm^{-1}). A broad peak was present in the SAXS region due to scattering from the lamellar morphology (Fig. 1). Scattering plots revealed a linear Porod region with a slope of approximately 4 at ultra-low q values indicating the presence of large micrometer-size scatterers with sharp interfaces such as voids in all samples (Fig. 1). The surface area to volume ratio (cm^{-1}) of void scatterers was calculated by

$$\frac{S}{V} = \frac{K}{2\pi\Delta\rho^2},$$

where S/V is the surface area to volume ratio of void scatters (cm^{-1}), K is the initial slope of the linear fit of q^2I plotted with respect to q^{-2}, and $\Delta\rho$ is the difference between electron densities of air and UHMWPE, respectively. Electron densities, ρ, were calculated by

$$\rho = \frac{[r]\left[\sum_1^n z_i\right][\rho_m][A]}{M},$$

where r is the classical radius of an electron ($2.81794E^{-13}$ cm), z_i is the number of electrons per atomic species, ρ_m is the density of either air or amorphous and crystalline UHMWPE (g/cm^3), A is the Avogadro's number (mol^{-1}), and M is the molecular weight (g/mol) of the species. The surface area to volume ratio of void scatters was $255 \pm 5\,cm^{-1}$ for all samples regardless of crystallization conditions.

Due to the presence of broad peaks, it was necessary to obtain long periods from paired distance distribution functions (PDDFs) or $p(r)$, which are identical to the one-dimensional correlation function for lamellar systems. USAXS scattering functions were converted to PDDFs using a previously established inverse Fourier transform technique and the computer program ITP developed by Glatter [22]. The PDDF is related to the scattering function $I(q)$ by the following equation:

$$p(r) = (1/2\pi^2 A)\int_0^\infty q^2 I(q)\cos(qr)\,dq,$$

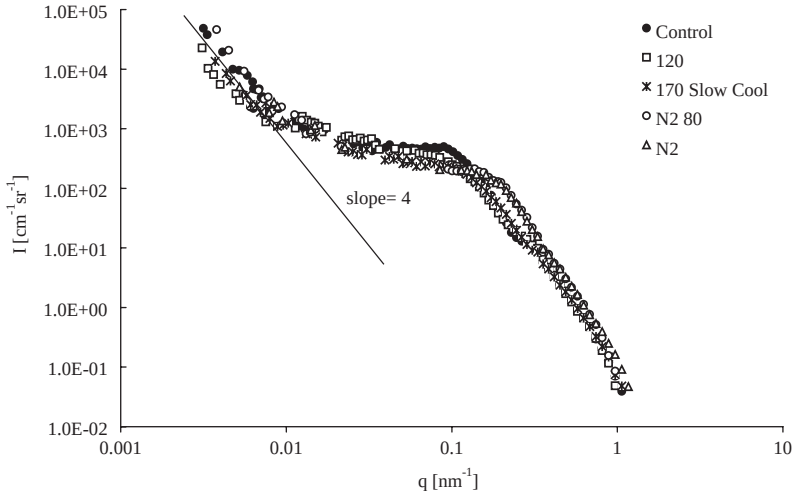

Fig. 1. USAXS scattering plot for all crystallization experiments and non-heat treated control UHMWPE.

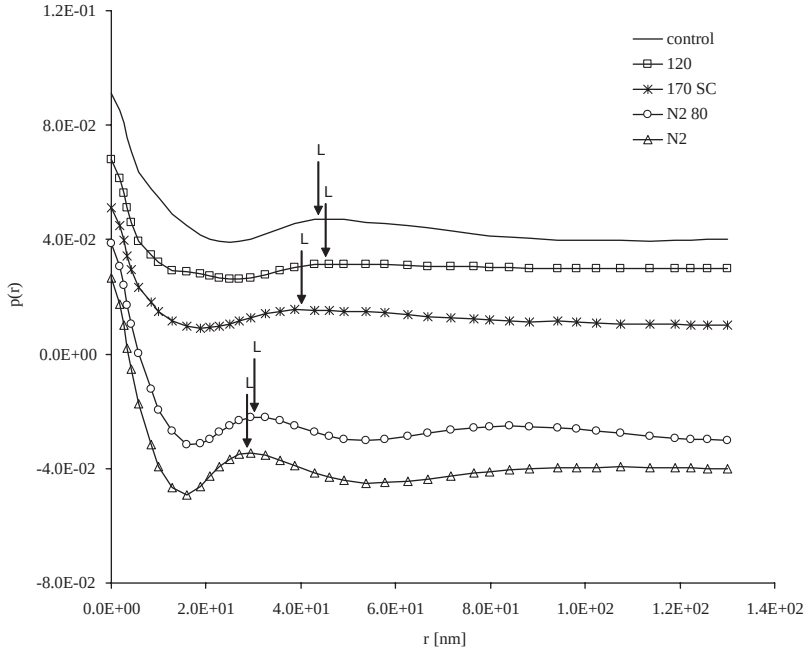

Fig. 2. PDDFs, $p(r)$, for all crystallization experiments and non-heat treated control UHMWPE. All PDDF curves have been offset for clarity. The indicated position of "L" represents the long period, or inter-lamellar spacing.

where $p(r)$ is the PDDF, A is the area of the lamella, $I(q)$ is the experimental scattering function, q is the scattering vector, and r is the radial distance perpendicular to lamellar surfaces within a stack of lamellae. PDDFs have previously been used to analyze the lamellar morphology of both medium molecular weight low-density polyethylene [23,24] as well as UHMWPE [2]. The USAXS long period (inter-lamellar spacing), L, for all samples was measured from the first maximum of $p(r)$ (Fig. 2). USAXS revealed that UHMWPE, which had been isothermally crystallized at 120°C, had the highest inter-lamellar spacing, followed by control UHMWPE and UHMWPE that had been slowly cooled from the melt. The long periods were observed to be smallest and nearly identical in quenched UHMWPE and quench/80°C UHMWPE (Tables 1 and 2).

PDDFs were also used to determine the specific internal surfaces (O_{ac}), or the area per unit volume of the interface separating the crystalline and the amorphous regions of all samples. Values of O_{ac} were determined using a previously established method [25,26] where

$$O_{ac} = \frac{-2dP/dr}{\Delta\rho_e^2}$$

Table 1
Characterization of the crystalline morphology of UHMWPE following crystallization experiments

Thermal history	X_c (%) DSC	L (nm) USAXS	D (nm) USAXS	A (nm) USAXS	O_{ac} 10^5 (cm^{-1}) USAXS	Q_{fit} 10^{12} (nm^{-4}) USAXS
Control	48.3	46.0	22.2	23.8	5.97	5.60
170°C/120°C 48 h	52.0	48.2	25.1	23.1	6.27	4.25
170°C slow cool	45.9	39.8	18.3	21.5	6.37	4.59
170°C/N_2/80°C 48 h	42.9	30.9	13.3	17.6	8.60	7.59
170°C/N_2	34.6	29.4	10.2	19.2	9.61	7.54

X_c—crystallinity ±3%, L—inter-lamellar spacing ±1.5 nm, D—lamellar thickness, A—amorphous region thickness, O_{ac}—specific internal surface, Q_{fit}—invariant.

Table 2
Mechanical properties of UHMWPE following crystallization experiments

Thermal history	Tensile modulus (MPa)	Yield stress (MPa)	Ultimate tensile stress (MPa)	True strain at break (mm/mm)	Work-of-fracture (MJ/mm^3)
Control	225.2±26.4	19.4±0.4	55.4±1.7	2.32±0.02	324.1±19.0
170°C/120°C 48 h	267.8±26.0	19.2±0.1	49.1±0.7	2.44±0.01	322.6±8.3
170°C slow cool	255.0±28.1	19.1±0.3	44.6±1.2	2.38±0.02	280.2±12.1
170°C/N_2/80°C 48 h	227.3±10.2	18.5±0.1	59.0±1.7	2.96±0.08	748.0±98.7
170°C/N_2	186.0±14.8	16.6±0.1	47.2±0.7	2.46±0.02	305.8±10.8

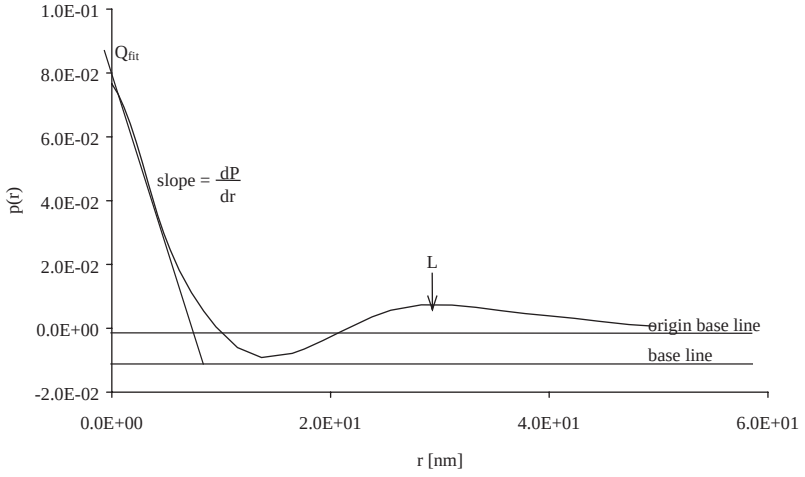

Fig. 3. Typical one-dimensional correlation function and associated parameters for lamellar systems.

such that dP/dr represents the slope of the linear fit to the self-correlation portion of the $p(r)$ function (Figs. 3 and 4) and $\Delta\rho_e$ is the difference in electron density between the crystalline and the amorphous regions of UHMWPE. The value of Q_{fit}, or the invariant, was determined from the y-intercept of the linear fit to the self-correlation portion of $p(r)$. Table 1 shows that the specific internal surfaces of the quenched UHMWPE had the highest specific internal surfaces. The 80°C annealing treatment of the quenched UHMWPE decreased its specific internal surface. The invariant of both rapidly quenched samples was also found to be high in comparison to the Q_{fit} value observed in all other sample groups.

3.2. Differential scanning calorimetry

A combination of DSC crystallinity and USAXS inter-lamellar spacings were used to determine both the thickness of crystalline lamellae and the amorphous regions. Lamellar thickness was calculated by

$$D = X_c L,$$

where D is the lamellar thickness, X_c is the degree of crystallinity (%) measured by DSC, and L represents the USAXS long period (inter-lamellar spacing). The thickness of the amorphous region (A) was calculated by taking the difference between the inter-lamellar spacing (L) and the lamellar thickness (D). Values for

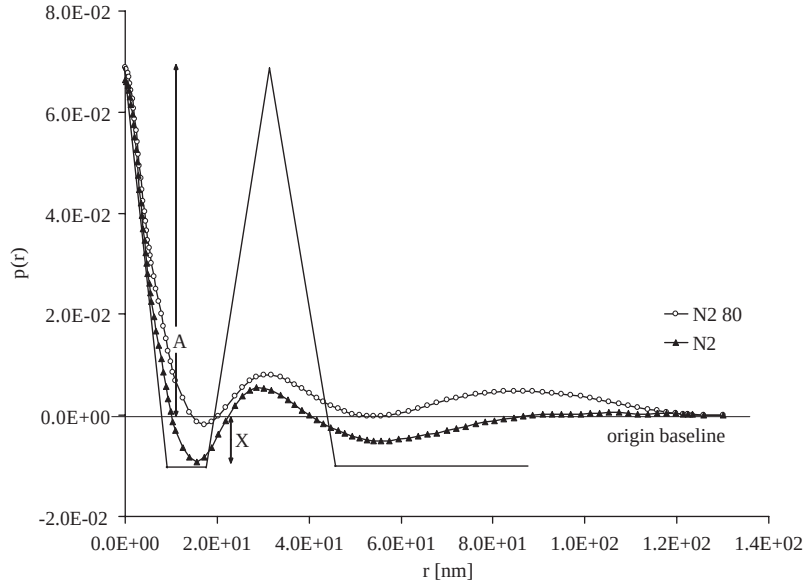

Fig. 4. PDDFs for rapidly quenched UHMWPE samples and the one-dimensional correlation function for the ideal lamellar model (curve a). Peaks for quenched samples are "dampened" due to deviations from the ideal lamellar model observed in actual samples. Area above the origin base line, *A*, represents the amorphous region while the area below the origin base line, *X*, represents the crystalline phase within the polymer sample.

DSC crystallinity, inter-lamellar spacing, crystalline and amorphous region thickness, and specific internal surfaces, O_{ac}, are reported in Table 1. Rapid cooling (quenching) of the melted UHMWPE resulted in the lowest degree of crystallinity and lamellar thickness. In contrast, the highest degree of crystallinity was obtained using isothermal crystallization at 120°C.

3.3. Low-voltage scanning electron microscopy

LVSEM micrographs revealed the presence of visibly thicker lamellae for UHMWPE that had been isothermally crystallized at 120°C, rod stock control UHMWPE and UHMWPE that had been slowly cooled from the melt state in comparison to quenched UHMWPE and quench/80°C UHMWPE (Figs. 5–8). There was no discernable difference in lamellar thickness between the quenched material and the quench/80°C UHMWPE. However, the overall number of lamellae, though they were smaller in size, was greater in both of the quenched UHMWPE samples compared to all other samples.

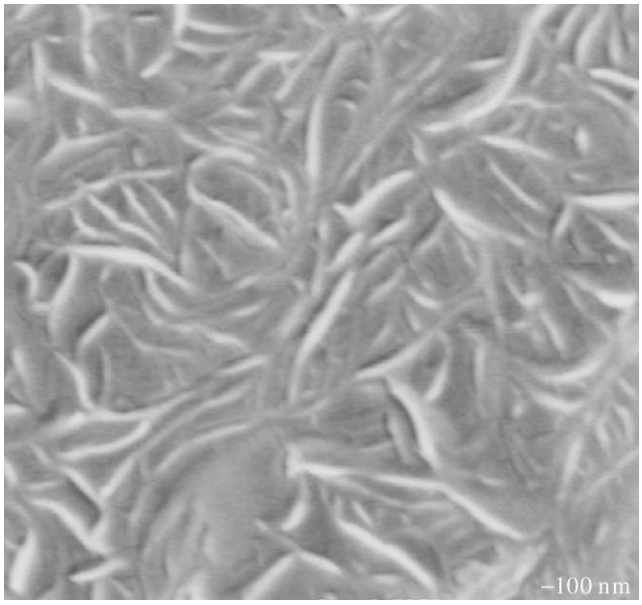

Fig. 5. LVSEM micrograph of permanganic acid etched freeze fracture surface of rod stock control UHMWPE (magnification = 40,000 ×, scale bar = 100 nm).

3.4. Mechanical tests

Uniaxial mechanical tests showed that in most cases, the morphological differences among samples were not accompanied by statistically significant differences in mechanical properties such as tensile modulus, yield stress, true strain and work-of-fracture. The differences in the tensile modulus between the isothermally crystallized (120°C), control and the slow cooled UHMWPE were not statistically significant. However, the tensile modulus of the quenched UHMWPEs was significantly lower than the tensile modulus of the isothermally crystallized UHMWPE (120°C), which was the highest. The highest UTS and WOF was observed in quench/80°C UHMWPE. The lower UTS observed in the slowly cooled UHMWPE, isothermally crystallized (120°C), and rapidly quenched material was statistically different

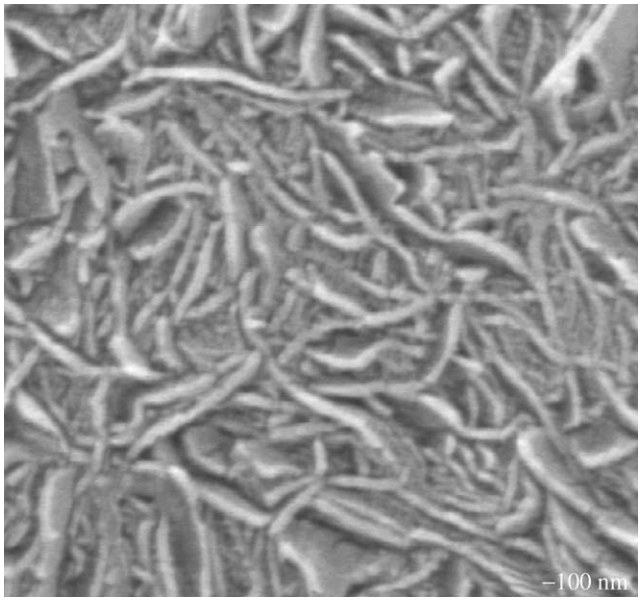

Fig. 6. LVSEM micrograph of permanganic acid etched freeze fracture surface of UHMWPE crystallized at a low undercooling temperature of 120°C (magnification = 40,000 ×, scale bar = 100 nm).

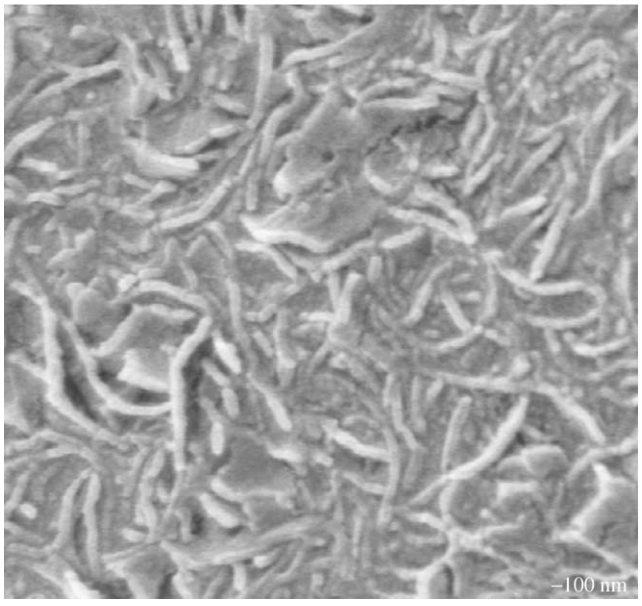

Fig. 7. LVSEM micrograph of permanganic acid etched freeze fracture surface of UHMWPE slowly cooled from the melt state (magnification = 40,000 ×, scale bar = 100 nm).

from both the control UHMWPE as well as the quench/80°C UHMWPE. ($p<0.05$, ANOVA with Fisher's PLSD post-hoc test). Additionally, the lower yield stress in the rapidly quenched UHMWPE compared to all other heat treatments was statistically significant. ($p<0.05$, ANOVA, with Fisher's PLSD post-hoc test).

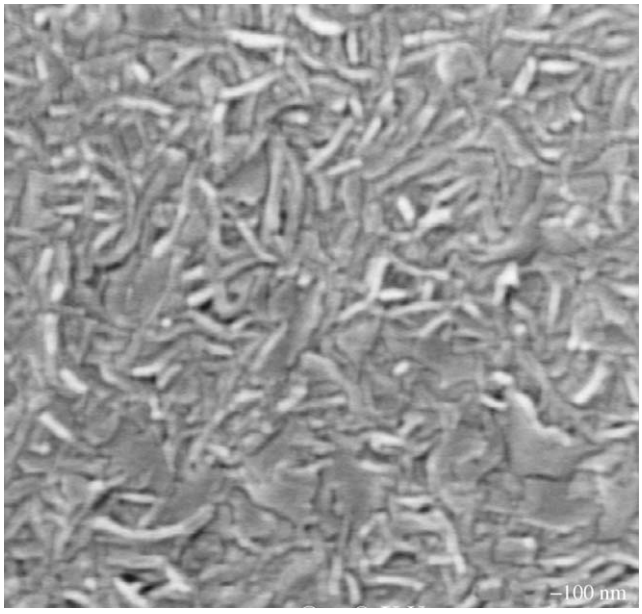

Fig. 8. LVSEM micrograph of permanganic acid etched freeze fracture surface of quenched UHMWPE (magnification = 40,000 ×, scale bar = 100 nm).

4. Discussion

The original hypothesis that UHMWPE morphology can be controlled by varying crystallization conditions, and that morphology would in turn influence the mechanical properties of UHMWPE was only partially confirmed by the results of this study. The crystallization conditions that were investigated strongly influenced the lamellar morphology of UHMWPE as was evidenced by characterization using USAXS, DSC, and LVSEM. Although it was possible to produce UHMWPEs with a range of morphologies by varying the crystallization conditions, in most cases the resulting differences in mechanical properties between UHMWPE samples were not significant.

LVSEM showed discernible evidence of the differences in lamellar thickening for samples that were isothermally crystallized (120°C) near the melting temperature of UHMWPE, rod stock control UHMWPE and for samples that were slowly cooled from the melt state in comparison to both rapidly quenched UHMWPE samples. USAXS provided supplementary quantitative characterization of variations in the lamellar morphology between UHMWPE samples. A comparison of the USAXS inter-lamellar spacings in combination with the overall degree of crystallinity provided by DSC showed that rapidly quenched UHMWPE had more than a 50% higher number of lamellae per unit volume compared to rod stock control UHMWPE. This result was expected since it is well known that rapid quenching increases the nucleation

density of UHMWPE, resulting in a larger number of thin lamellae. In contrast, slow cooling or isothermal crystallization near the melting temperature generally induces a relatively higher degree of crystallinity but with an overall smaller number of thick lamellae [6]. In addition, it is well known that rod stock is subjected to pressure during ram extrusion, which also results in the presence of thick lamellae.

USAXS PDDF plots also provided differences in lamellar and amorphous region thickness, spacing between lamellae, and the specific internal surfaces associated with the interface separating the crystalline and the amorphous regions of all samples. Interestingly, in the case of both rapidly quenched UHMWPEs, nearly identical USAXS long periods were observed. However, the quench/80°C UHMWPE showed an approximate 30% increase in DSC crystallinity compared to UHMWPE that had been quenched with no further heat treatment. Closer examination of their corresponding PDDFs (see Fig. 4) provides more insight into the alteration in lamellar morphology with annealing at 80°C after rapid quenching in liquid nitrogen. The *y*-intercept of the PDDF curve above the origin base line (Fig. 4) is taken to represent the amorphous region, marked by "*A*" in Fig. 4. Similarly, "*X*" is a measure of the crystalline region [27]. However, unlike medium molecular weight polyethylenes, in the case of UHMWPE, there is overlap between initial linear decay of the PDDF and the first peak associated with the long period. Thus, it is difficult to measure the correct value of "*X*" for all of these UHMWPE samples. The value of "*X*" can only be estimated using DSC. Another observation is the differences in the slope of the initial linear region of the PDDFs, which is a measure of the specific internal surface, or O_{ac}. The decrease in O_{ac} due to annealing at 80°C (see Table 1) is probably due to the fact that heating the quenched samples to 80°C destroys some nuclei so that the overall nucleation density for the quench/80°C UHMWPE is lower than for the quenched UHMWPE with no subsequent annealing. The overall observed increase in crystallinity in the case of the quench/80°C UHMWPE is consistent with another feature of the PDDF curve, the invariant. While the position of the first peak of the PDDF curve (used to determine the value of the USAXS long period) was nearly identical for both samples, the invariant (Q_{fit}) for quench/80°C UHMWPE was higher than the observed Q_{fit} in the sample that had been quenched with no further heat treatment (Table 1). The PDDF of the quenched samples also showed evidence for a second broad peak in the 80–100 nm region (see Figs. 3 and 4), probably due to scattering from the width dimension of the ill-formed, "ribbon-like" lamellae associated with quenched UHMWPE. A higher invariant suggests crystallinity values closer to 50%, as the invariant is at a maximum at 50% (due to the relationship of $x(1-x)$, where "*x*" represents crystallinity) [27]. The nearly identical values of *L* for both quenched samples suggests that while the inter-lamellar spacing of these particular samples was similar, the isothermally crystallized sample was comprised of thicker lamellae resulting from isothermal crystallization. The finding that crystallinity increases while the long period remains almost constant, as in the case of the quench/80°C UHMWPE, is in agreement with the results of earlier research that concluded that crystallinity increases at the expense of the amorphous phase [28,29]. An unexpected result from the analysis of PDDFs was that the two rapidly quenched samples showed higher Q_{fit} values in comparison to all other sample groups. This discrepancy could perhaps be attributed to the presence of a transition layer that forms in material that is isothermally crystallized (120°C) just below the melt and slowly cooled UHMWPE. The formation of a transition layer between crystalline and amorphous phases would tend to suppress Q_{fit} as the value of the invariant decreases as the width of the transition layer increases [27]. The process of rapid quenching may preclude the formation of a transition layer thereby unaffecting the value of its Q_{fit} relative to the other crystallization conditions investigated in this study. In this study, UHMWPE that was isothermally crystallized at 120°C produced the highest overall crystallinity. This occurred due to the slow kinetics of crystallization that is expected when polyethylene is annealed at temperatures slightly below the melting point. As a consequence, the polymer chains had more time to disentangle and to be incorporated into the growing lamellae.

As previously mentioned, differences in morphology in most cases did not produce corresponding differences in mechanical properties. Quenching results in the formation of a greater number of tie-molecules compared to slow cooling. These "ties" would be expected to behave as "physical crosslinks" yielding tougher UHMWPE products. While some studies have demonstrated this phenomenon [3], conversely, others have noted a decrease in yield stress and modulus. Truss et al. [5] showed that slow cooling UHMWPE from 142°C in nitrogen produced a material that had a modulus of 475 MPa and a yield strength of 21.7 MPa, whereas water quenching following 200°C temperatures produced UHMWPE with a modulus of only 213 MPa and a yield strength of 13.8 MPa. Their result is consistent with this study, which also showed a significant reduction in both yield stress and modulus for the liquid nitrogen quenched UHMWPEs. It should be noted that the quench/80°C UHMWPE exhibited the highest UTS, a result that was statistically significant in comparison to UHMWPE that was slowly cooled, isothermally crystallized at 120°C, and quenched without further heat treatment ($p<0.05$, ANOVA, with Fisher's PLSD post-hoc test). In fact, the UTS of

quench/80°C UHMWPE was 25% higher than that of UHMWPE that was quenched with no further heat treatment. Additionally, the WOF for quench/80°C UHMWPE was more than twice the WOF for UHMWPE that was quenched with no further application of heating treatments. These observations are probably due to the differences in the quantity and the size of lamellae of the quench/80°C UHMWPE, as well as the conformation of chains in the amorphous regions.

5. Conclusions

This study revealed that the effect of morphology on mechanical properties was not significant for most of the crystallization conditions investigated. The increase in UTS, WOF, and True Strain at Break observed in the quench/80°C UHMWPE requires further investigation of quenched/annealed UHMWPEs. Such a study would provide more insight into the relationship between number of lamellae, their thickness and the corresponding macroscopic mechanical properties of these materials. It must be noted however, that in the context of wear testing, the low thermal conductivity of UHMWPE can only allow an approximately 0.5–1 mm deep subsurface region of the articular surface to be modified by the rapid quenching process while the bulk material will crystallize slowly. While this study helped to elucidate that morphology can be systematically modified by controlling crystallization conditions, a more comprehensive structure-property-processing study would be necessary, in order to determine the ideal crystallization conditions needed to develop orthopaedic implants with superior mechanical performance.

Acknowledgements

This study was supported by a biomedical engineering grant by the Whitaker Foundation. The expert assistance of Dr. Peter Jemian and Dr. Jan Ilavsky with USAXS measurements is greatly appreciated. The UNICAT facility at the Advanced Photon Source (APS) is supported by the University of Illinois at Urbana Champaign, Materials Research Laboratory (US Department of Energy, the State of Illinois-IBHE-HECA, and the National Science Foundation), the Oak Ridge National Laboratory (US Department of Energy), the National Institute of Standards and Technology (US Department of Commerce), and UOP LLC. The APS is supported by the US Department of Energy, Office of Science, Office of Basic Energy Sciences, under Contract No. W-31-109-ENG-38. In addition, we thank Michael Frongillo at the Center for Material Science and Engineering at the Massachusetts Institute of Technology for his expert assistance with SEM. This work made use of MRSEC Shared Experimental Facilities supported by the National Science Foundation under award number DMR98-08941.

References

[1] Kurtz SM, Muratoglu OK, Evans M, Edidin AA. Advances in the processing sterilization and crosslinking of ultra-high molecular weight polyethylene for total joint arthroplasty. Biomaterials 1999;20:1659–88.
[2] Bellare A, Schnablegger H, Cohen RE. A small-angle X-ray scattering study of high-density polyethyelene and ultra-high molecular weight polyethylene. Macromolecules 1995;17:2325–33.
[3] Arends CB. Polymer toughening. New York: Marcel Dekker; 1996. p. 190–1.
[4] Phillips PJ. Polymer crystals. Rep Prog Phys 1990;53:549.
[5] Truss RW, Han KS, Wallace JF, Geil PH. Cold compaction molding and sintering of ultra-high molecular weight polyethylene. Polym Eng Sci 1980;20:747–55.
[6] Voigt-Martin IG, Fisher EW, Mandelkern L. Morphology of melt-crystallized linear polyethylene fractions and its dependence on molecular weight and crystallization temperature. J Polym Sci (Polym Phys) 1980;18:2347–67.
[7] Bassett DC, Carder DR. Oriented chain-extended polyethylene. 1. Formation and characterization. Philos Mag 1973;8:513–33.
[8] Rees DV, Bassett DC. Origin of extended-chain lamellae in polyethylene. Nature 1968;219:368–70.
[9] Rees DV, Bassett DC. On the formation of extended-chain lamellae in polyethylene. J Polym Sci (B) 1969;7:273–80.
[10] Ramani K, Parasnis NC. Process-induced effects in compression molding of ultra-high molecular weight polyethylene (UHMWPE). In: Gsell RA, Stein HL, Ploskonka JJ, editors. Characterization and properties of ultra-high molecular weight polyethylene. West Conshohoken: American Society for Testing and Materials; 1998. p. 5–23.
[11] Wang X-Y, Li S-Y, Salovey R. Processing of ultra-high molecular weight polyethylene. J Appl Polym Sci 1988;35:2165–71.
[12] Bellare A, Cohen RE. Morphology of rod stock and compression-moulded sheets of ultra-high-molecular-weight polyethylene used in orthopaedic implants. Biomaterials 1996;17:2325–33.
[13] Bastiaansen CWM, Meyer HEH, Lemstra PJ. Memory effects in polyethylenes: influence of processing and crystallization history. Polymer 1990;31:1435–40.
[14] Zachariades AE. The effect of powder particle fusion on the mechanical properties of ultra-high molecular weight polyethylene. Polym Eng Sci 1985;25:747–50.
[15] Gul, R. Improved UHMWPE for use in total joint replacement. PhD Dissertation. Boston: Massachusetts Institute of Technology; 1997.
[16] Pruitt L, Bailey L. Factors affecting the near-threshold fatigue behavior of surgical grade ultra high molecular weight polyethylene. Polymer 1998;39:1545–53.
[17] Johnson T, Devanathan D, Swarts D, King R, Lin S, Gsell R, Rohr W. Process dependent characteristics of polyethylene. In: Transactions of the Fifth World Biomaterials Congress, vol. 2, 1996. p. 514.
[18] Wunderlich B. In: macromolecular physics, vol. 1. New York: Academic press; 1973. p. 388.
[19] Olley RH, Bassett DC. An improved permanganic etchant for polyolefines. Polym Commun 1982;23:1707–10.
[20] Olley RH, Hodge MA, Bassett DC. A permanganic etchant for polyolefines. J Polym Sci 1979;17:627–43.

[21] Olley RH, Hosier IL, Bassett DC, Smith NG. On morphology of consolidated UHMWPE resin in hip cups. Biomaterials 1999;20:2037–46.
[22] Glatter O. Data evaluation in small-angle scattering: calculation of the radial electron density by means of indirect Fourier transformation. Acta Phys Austriaca 1977;47: 83–102.
[23] Strobl GR, Schneider M. Direct evaluation of the electron density correlation function of partially crystalline polymers. J Polym Sci: Polym Phys Ed 1980;18:1343–59.
[24] Strobl GR, Schneider MJ, Voigt-Martin IG. Model of partial crystallization and melting derived from small angle X-ray scattering and electron microscopic studies on low density polyethylene. J Polym Sci: Polym Phys Ed 1980;18:1361.
[25] Schmidtke J, Strobl G, Albrecht T. A four-state scheme for treating polymer crystallization and melting suggested by calorimetric and small angle X-ray scattering experiments on syndiotactic polypropylene. Macromolecules 1997;30:5804–21.
[26] Albrecht T, Strobl G. Observation of the early stages of crystallization in polyethylene by time-dependent SAXS: transition from individual crystals to stacks of lamellae. Macromolecules 1996;29:783–5.
[27] Vonk CG. Synthetic polymers in the solid state. In: Glatter O, Kratky O, editors. Small angle X-ray scattering. London: Academic Press; 1982.
[28] Albrecht T, Strobl G. Temperature-dependent crystalline-amorphous structures in linear polyethylene: surface melting and the thickness of the amorphous layers. Macromolecules 1995;28: 5827–33.
[29] Rieger J, Mansfield M. Comments on ''temperature-dependent changes in the structure of the amorphous domains of semicrystalline polymers''. Macromolecules 1989;22:810–3812.